CONSTRAINTS ON PRIMORDIAL MAGNETIC FIELDS WITH PLANCK 2015

Daniela Paoletti - INAF/IASF and INFN Bologna

&

The Planck Collaboration

December 2015, Texas Symposium, Geneve

SCIENTIFIC CASE

Magnetic fields generated in the early universe may represent initial seeds which may contribute to the generation of the large scale magnetic fields.

See Durrer & Neronov for a review

Magnetic fields generated in the early universe –therefore present even without an associated structure -provide an interpretations of the lack of photons measured by Fermi in a Blazar. *Neronov & Vovk 1010, Tavecchio et al. 2010, Taylor et al. 2011,Vovk et al. 2012*

The early universe can naturally generate magnetic fields. Either during inflation or afterwards during phase transitions or recombination. *Vachaspati 1991,Joyce & Shaposhnikov 1997, Giovannini & Shaposhnikov 2000, Martin & Yokoama 2007, Demozzi et al. 2009,Turner & Widrow 1988, Garretson, Field & Carroll 1992, Finelli & Gruppuso 1999, Calzetta & Kandus 2002, Garcia Bellido et al. 2008, Byrnes et al. 2012,Ratra 1988, Gasperini, Giovannini & Veneziano 1995….*

Different mechanism=Different characteristics

PRIMORDIAL MAGNETIC FIELDS (PMF) LIKE A GOOD WINE ARE BECOMING MORE AND MORE INTERESTING WITH PASSING TIME

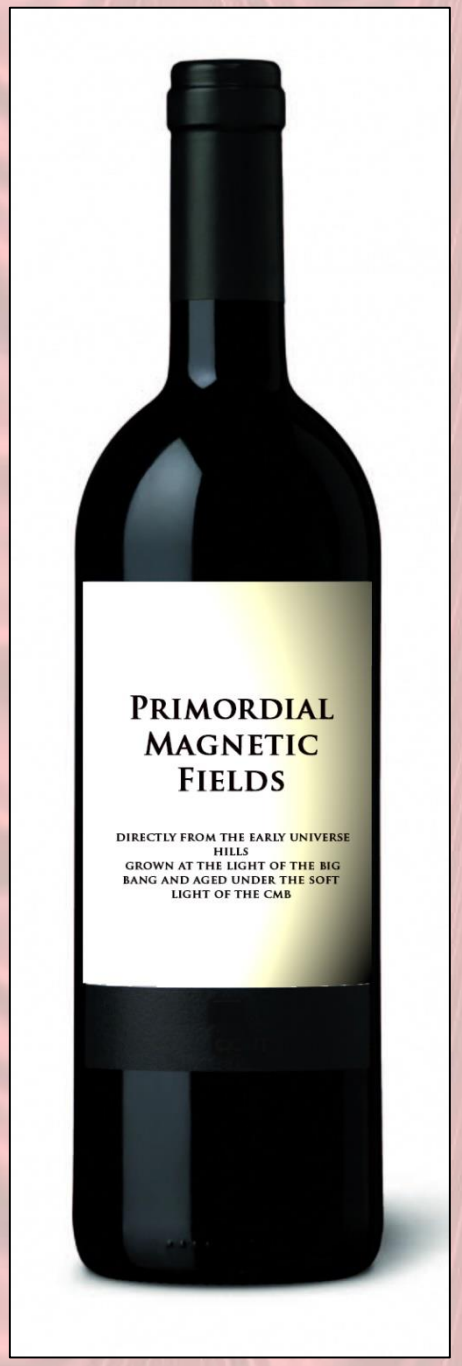

THE CMB AND THE PMF

PMF affect CMB anisotropies in different ways

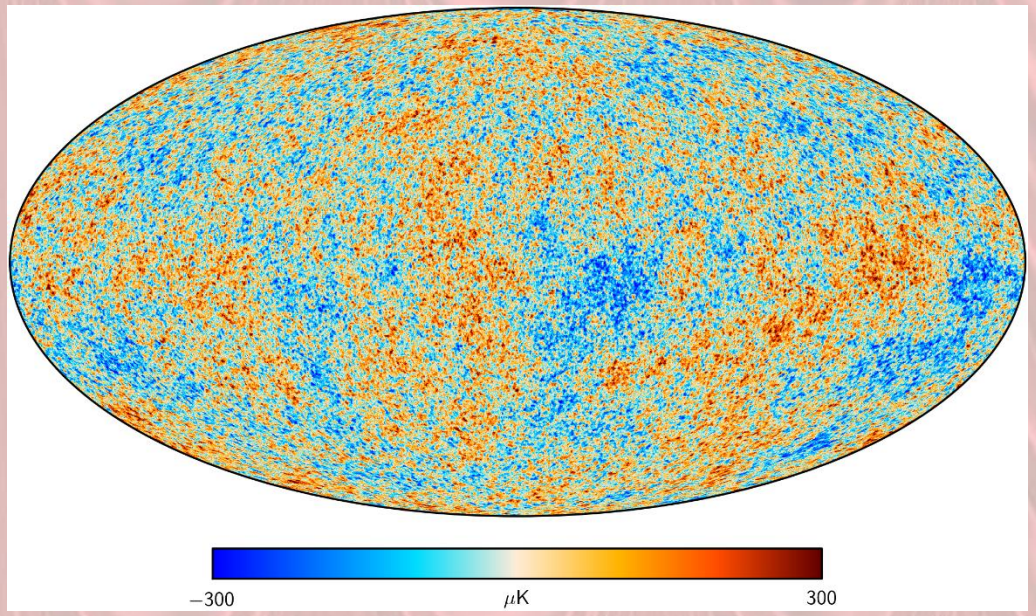

Planck 2015 foreground cleaned SMICA map

PMF modify the evolution of cosmological perturbations and have a direct effect on CMB anisotropies

CMB anisotropies thanks to the variety of probes in a single observable, are one of the best laboratory to investigate PMF

PMF induce a Faraday rotation of the CMB anisotropies in polarization

PMF modelled as a stochastic background have a fully non-Gaussian impact on CMB anisotropies

One of the main tools to constrain PMF with CMB anisotropies are the CMB angular power spectra

Planck 2015 Temperature APS

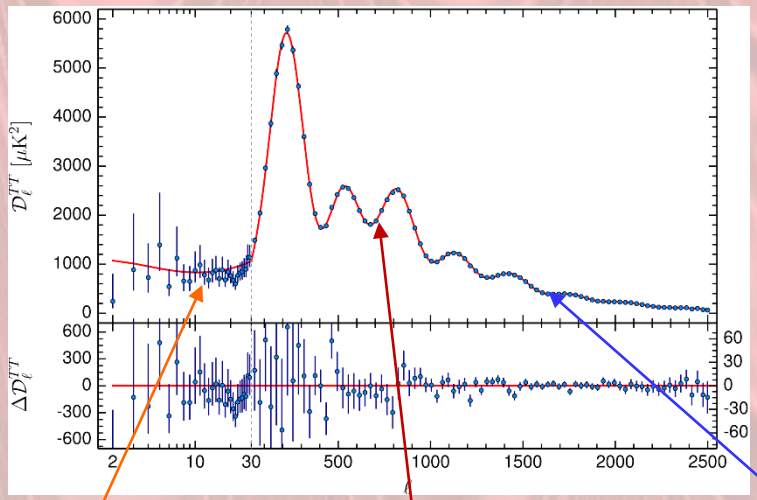

Planck 2015 E-mode

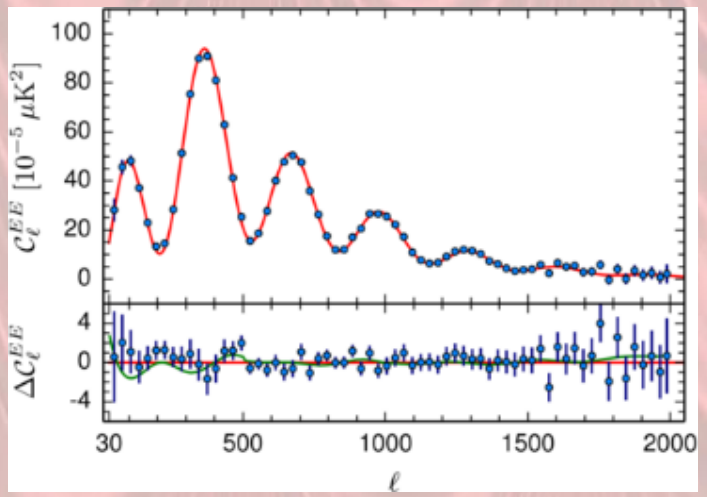

Large angular scales are scales outside the horizon at recombination.

Small angular scales
Data contamination by astrophysical signals

Intermediate scales
Acoustic oscillations of the photon baryon fluid.

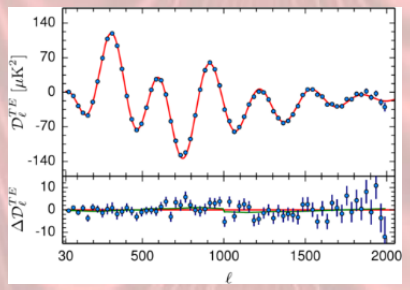

Planck 2015 cross correlation Temperature-E-mode

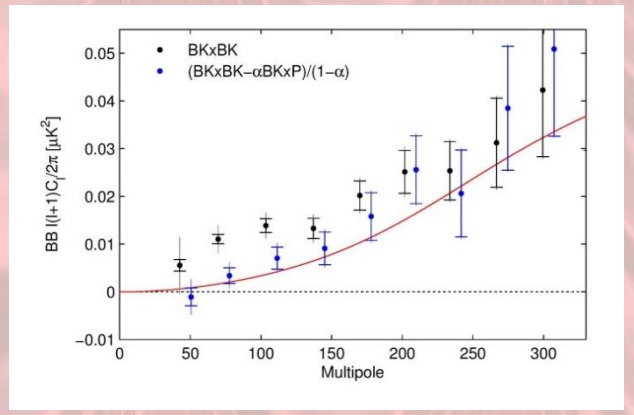

Planck+BICEP 2+KECK B-mode (blue points, black are the original BKxBK data)

PMF MODELLED AS A STOCHASTIC BACKGROUND.
WE NEGLECT ALL THE CONTRIBUTIONS TO THE BACKGROUND.

PMF source all types of perturbations:

SCALAR

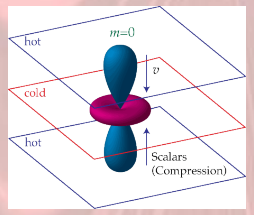

Credits Wayne Hu
http://background.uchicago.edu/

Standard perturbations in the energy density and pressure of the cosmological fluid.

SOURCED BY ENERGY DENSITY AND ANISOTROPIC STRESS

VECTOR

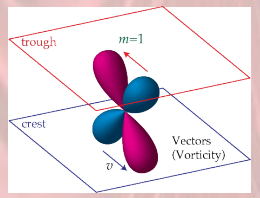

Represent the vortical motions of matter in the plasma. The standard vector mode sourced by neutrinos is in fact a decaying mode.

SOURCED BY ANISOTROPIC STRESS

TENSOR

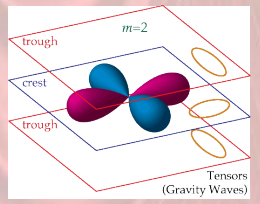

Tensor perturbations are traceless and transverse metric perturbations and are a key prediction of many inflationary models.

SOURCED BY ANISOTROPIC STRESS

If you see a B-mode..would you be sure to be seeing primordial gravitational waves?

Cosmological perturbations are described by the coupled system of Einstein equations for metric perturbations and the Boltzmann equations for the fluid perturbations.
PMF are an additional component to the plasma but their contribution to the background is negligible.

$$\delta G_{\mu\nu} = 8\pi(\delta T_{\mu\nu} + \tau_{\mu\nu}^{PMF})$$

PERTURBED METRIC TENSOR

FLUID PERTURBED ENERGY MOMENTUM TENSOR

MAGNETIC ENERGY MOMENTUM TENSOR

$$\tau_0^0 = -\rho_B = -\frac{|\vec{B}|^2}{8\pi G}$$
$$\tau_i^0 = \frac{\vec{E}\times\vec{B}}{8\pi G} = 0$$
$$\tau_j^i = \frac{1}{4\pi G}\left(\frac{|\vec{B}|^2}{2}\delta_j^i - \vec{B}^i\vec{B}_j\right)$$

Lorentz force term in baryons equations

$$\nabla_\mu \delta T^{\mu\nu} \propto F^{\mu\nu} J_\mu$$

Indirect effect of the Lorentz force also on photons during the tight coupling

PMF are an additional independent source therefore they generate independent magnetically induced modes

THE PMF EMT IS THE KEY TO MAGNETIC PERTURBATIONS

PRIMORDIAL MAGNETIC FIELDS ENERGY MOMENTUM TENSOR

$$\langle B_i(k) B_j^*(k') \rangle = \frac{(2\pi)^3}{2} \delta^{(3)}(k - k') \left[(\delta_{ij} - \hat{k_i}\hat{k_j}) P_B(k) + i\, \epsilon_{ijl} \hat{k_l}\, P_H(k) \right]$$

Power-law power spectrum
for both helical and non-helical parts

$$P_B(k) = A_B\, k^{n_B}$$

$$P_H(k) = A_H\, k^{n_H}$$

Magnetized perturbations survive silk damping but are suppressed on smaller scales. *Subramanian and Barrow 1997, Jedamzik et al 1997*

$$k_D = (2.9 \times 10^4)^{\frac{2}{n_B+5}} \left(\frac{B_\lambda}{nGauss} \right)^{\frac{-2}{n_B+5}} \left(\frac{k_\lambda}{1 Mpc^{-1}} \right)^{\frac{n_B+3}{n_B+5}} \Omega_b h^2 Mpc$$

We modelled this damping with a sharp cut off in the PMF spectra

$$\langle \vec{B}_i^*(\vec{k}) \vec{B}_j(\vec{k'}) \rangle = \begin{cases} \delta^3(\vec{k} - \vec{k'})(\delta_{ij} - \hat{k}_i \hat{k}_j) \frac{P_B(k)}{2} & \text{for} \quad k < k_D \\ 0 & \text{for} \quad k > k_D \end{cases}$$

In the primordial universe we can assume the MHD limit and neglect backreaction of the fluid onto the fields

$$\rho_B(x,\tau) = \frac{\rho_B(x)}{a^4(\tau)} \rightarrow B(x,\tau) = \frac{B(x)}{a^2(\tau)}$$

Magnetic energy density simple evolution with the universe expansion

NOTATION

RMS OF THE FIELDS

$$\langle B^2(x)\rangle = \int_{k<k_D} d^3k P_B(k) = \frac{4\pi A}{n_B+3}\frac{k_D^{n_B+3}}{k_*^{n_B}}$$

SMOOTHED FIELDS

$$\langle B_\lambda^2(x)\rangle = \int d^3k e^{-\lambda^2 k^2} P_B(k) = 2\pi A \frac{\Gamma\left(\frac{n_B+3}{2}\right)}{\lambda^{n_B+3}}$$

HELICAL COMPONENT

$$\langle \mathcal{B}_\lambda^2\rangle = \lambda \int_0^\infty \frac{\mathrm{d}k\, k^3}{2\pi^2} \mathrm{e}^{-k^2\lambda^2} |P_H(k)| = \frac{|A_H|}{4\pi^2 \lambda^{n_H+3}} \Gamma\left(\frac{n_H+4}{2}\right)$$

n_B >-3 to avoid divergences

The energy momentum tensor power spectrum in Fourier space is given by very complex convolutions of the fields…

We need to compute the scalar, vector an tensor projections

$$\langle \tau_{ab}^*(\boldsymbol{k})\tau_{cd}(\boldsymbol{k}')\rangle = \int \frac{\mathrm{d}\boldsymbol{q}\,\mathrm{d}\boldsymbol{p}}{64\pi^5}\delta_{ab}\delta_{cd}\langle B_l(\boldsymbol{q})B_l(\boldsymbol{k}-\boldsymbol{q})B_m(\boldsymbol{p})B_m(\boldsymbol{k}'-\boldsymbol{p})\rangle$$
$$- \int \frac{\mathrm{d}\boldsymbol{q}\,\mathrm{d}\boldsymbol{p}}{32\pi^5}\langle B_a(\boldsymbol{q})B_b(\boldsymbol{k}-\boldsymbol{q})B_c(\boldsymbol{p})B_d(\boldsymbol{k}'-\boldsymbol{p})\rangle .$$

PMF EMT FOURIER SPECTRA

For CMB anisotropies the dominant contribution comes from small wavenumber-> infrared part of the spectra

INFRARED BEHAVIOUR

$$n > -3/2 \rightarrow white \quad noise$$

$$n < -3/2 \rightarrow k^{(2n+3)}$$

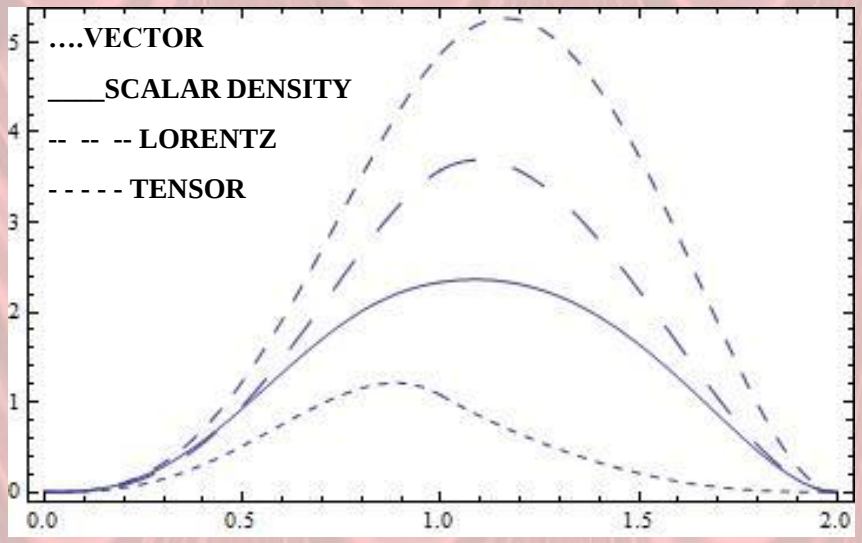

$$|\rho_B(k)|^2_{n_B=2} = \frac{A^2 k_D^7}{512\pi^4 k_*^4}\left[\frac{4}{7} - \tilde{k} + \frac{8\tilde{k}^2}{15} - \frac{\tilde{k}^5}{24} + \frac{11\tilde{k}^7}{2240}\right],$$

$$|\Pi_B^{(V)}(k)|^2_{n_B=2} = \frac{A^2 k_D^7}{256\pi^4 k_*^4}\left[\frac{4}{15} - \frac{5\tilde{k}}{12} + \frac{4\tilde{k}^2}{15} - \frac{\tilde{k}^3}{12} + \frac{7\tilde{k}^5}{960} - \frac{\tilde{k}^7}{1920}\right],$$

$$|\Pi_B^{(T)}(k)|^2_{n_B=2} = \frac{A^2 k_D^7}{256\pi^4 k_*^4}\left[\frac{8}{15} - \frac{7\tilde{k}}{6} + \frac{16\tilde{k}^2}{15} - \frac{7\tilde{k}^3}{24} - \frac{13\tilde{k}^5}{480} + \frac{11\tilde{k}^7}{1920}\right].$$

$$|L(k)|^2_{n_B=2} = \frac{A^2 k_D^7}{512\pi^4 k_*^4}\left[\frac{44}{105} - \frac{2\tilde{k}}{3} + \frac{8\tilde{k}^2}{15} - \frac{\tilde{k}^3}{6} - \frac{\tilde{k}^5}{240} + \frac{13\tilde{k}^7}{6720}\right].$$

Paoletti et Al: 2009

HELICAL COMPONENTS IN THE EMT

$$
\begin{aligned}
\left|\rho_B(k)\right|^2 &= \left|\rho_B(k)\right|^2_{\text{non-helical}} \\
&\quad -\frac{1}{512\pi^5}\int_\Omega d^3p\, P_H(p)\, P_H(\left|\boldsymbol{k}-\boldsymbol{p}\right|)\,\mu\,, \\
\left|L_B^{(S)}(k)\right|^2 &= \left|L_B^{(S)}(k)\right|^2_{\text{non-helical}} \\
&\quad +\frac{1}{64\pi^2 a^8}\int d^3p\, p\, P_H(p)\, P_H(\left|\boldsymbol{k}-\boldsymbol{p}\right|)\,(\mu-2\gamma\beta) \\
\left|\Pi^{(V)}(k)\right|^2 &= \left|\Pi^{(V)}(k)\right|^2_{\text{non-helical}} \\
&\quad +\frac{1}{512\pi^5}\int_\Omega d^3p\, P_H(p)\, P_H(\left|\boldsymbol{k}-\boldsymbol{p}\right|)\,(\mu-\gamma\beta) \\
\left|\Pi^{(T)}(k)\right|^2 &= \left|\Pi^{(T)}(k)\right|^2_{\text{non-helical}} \\
&\quad +\frac{1}{128\pi^5}\int_\Omega d^3p\, P_H(p)\, P_H(\left|\boldsymbol{k}-\boldsymbol{p}\right|)\,\gamma\left(1+\beta^2\right)
\end{aligned}
$$

$k^3|\rho(k)|^2$ in units of $\langle B^2\rangle^2/(4\pi)^4$ ($\langle \mathcal{B}^2\rangle^2/(4\pi)^4$)

n_B (n_H) = -3/2, -1, 0, 1, 2, 3, 4 ranging from the solid to the longest dashed

Non-Helical

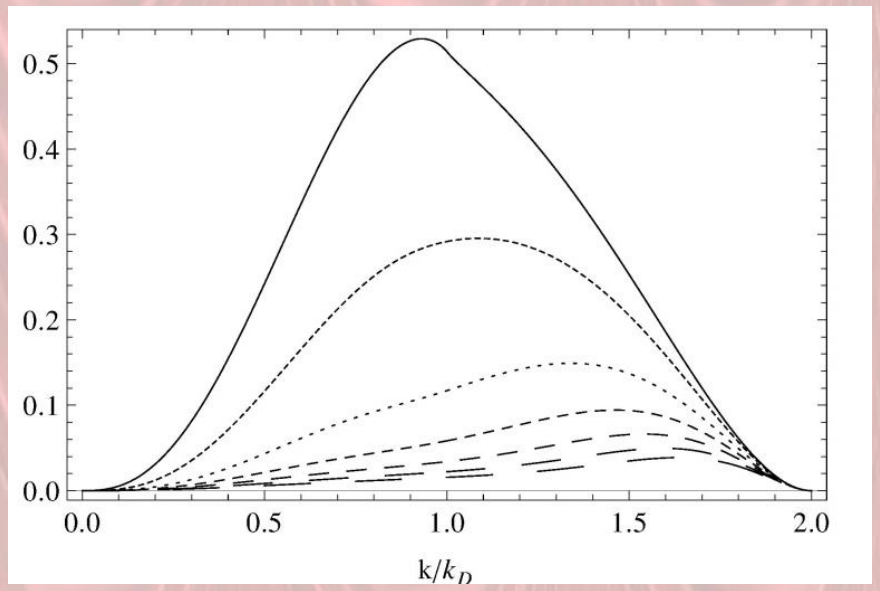

Helical

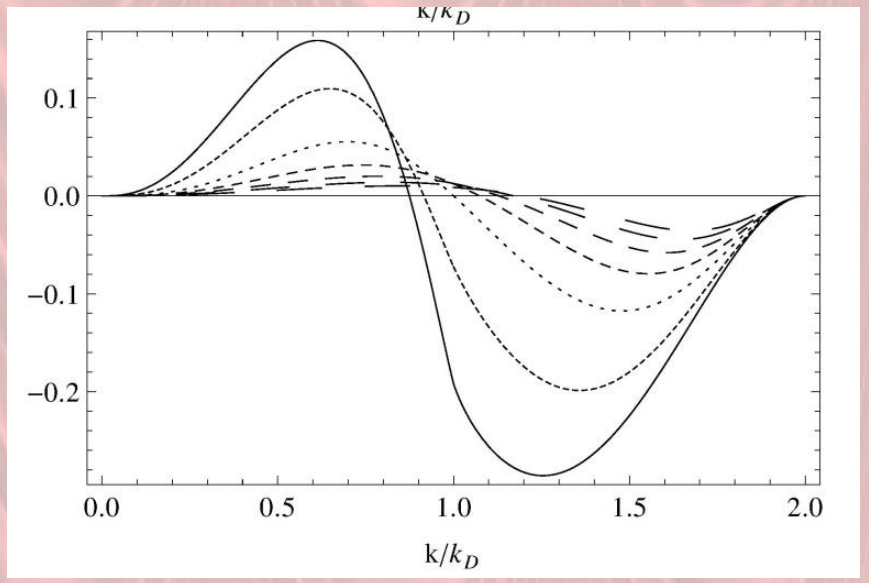

Non-Helical vs Maximum Helical

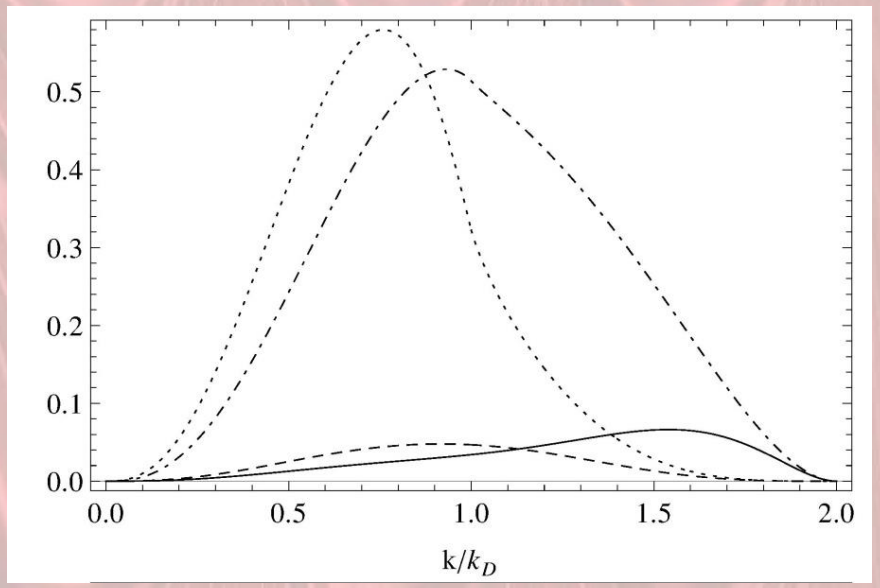

$n_{B,H} = -3/2$ (dot-dashed vs dotted).
$n_{B,H} = 1$ (solid vs dashed)

Non-helical vs max helical

Ballardini, Finelli and Paoletti 2015

MAGNETICALLY INDUCED ANGULAR POWER SPECTRA

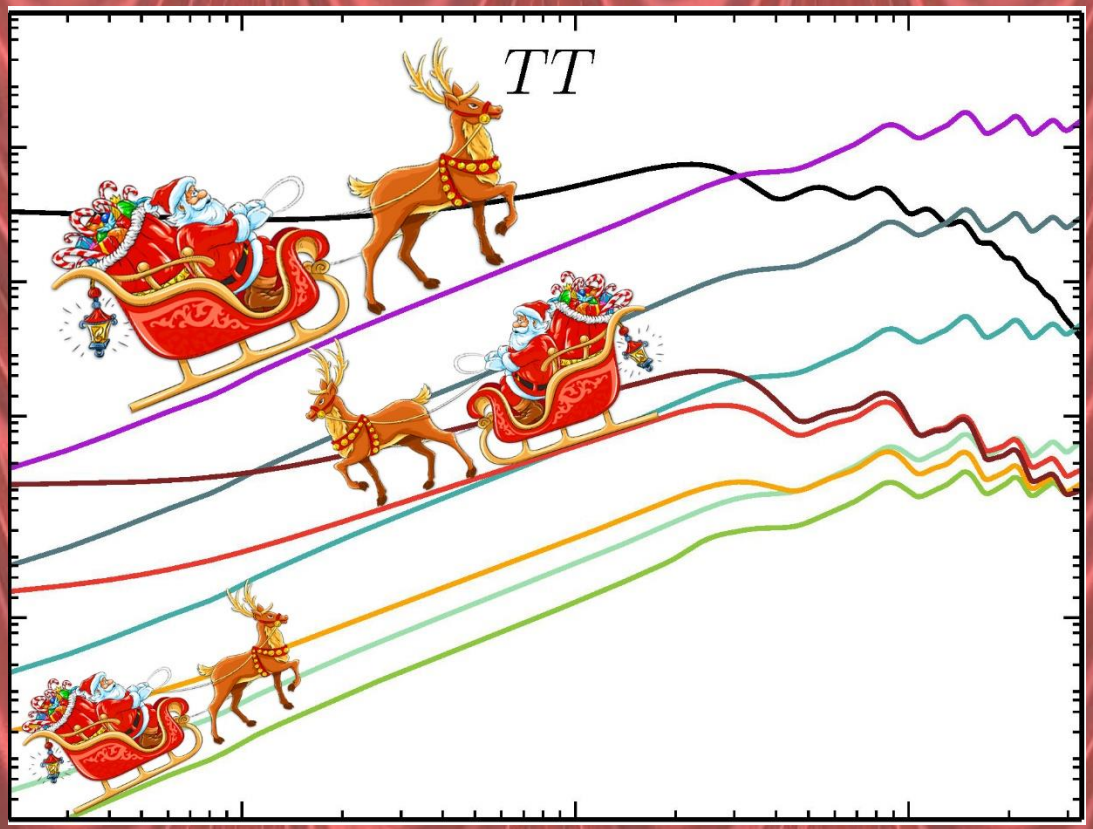

INITIAL CONDITIONS

Magnetically induced perturbations does not only come with different modes -scalar, vector and tensors- but also with different initial conditions.
Different initial conditions source different perturbations

- **Compensated:** Magnetically induced modes which are sourced by PMF energy mometum tensor after neutrino decoupling. The «compensated» definition comes from the compensation of magnetic terms by the fluid perturbations *(Giovannini 2004, Lewis 2004, Finelli et al. 2008, Paoletti et al. 2009, Shaw & Lewis 2010).*

- **Passive:** This mode is generated prior to the neutrino decoupling when the anisotropic stress of PMF has no counterpart in the fluid. This uncompensated source gives rise to an extra solution, logarithmic in time. After neutrino decoupling with the rise of their anisotropic stress, which compensates the PMF one, this solution no longer exists. But it leaves a footprint in the form of an offset in the amplitude of the inflationary mode for scalar and tensor perturbations *(Lewis 2004, Shaw and Lewis 2010).*

- **Inflationary:** This mode is strictly related to inflationary generated fields and is strongly dependent on the generation mechanism of the fields *(Bonvin et al. 2011,2013).*

NON-HELICAL MAGNETICALLY INDUCED ANGULAR POWER SPECTRA

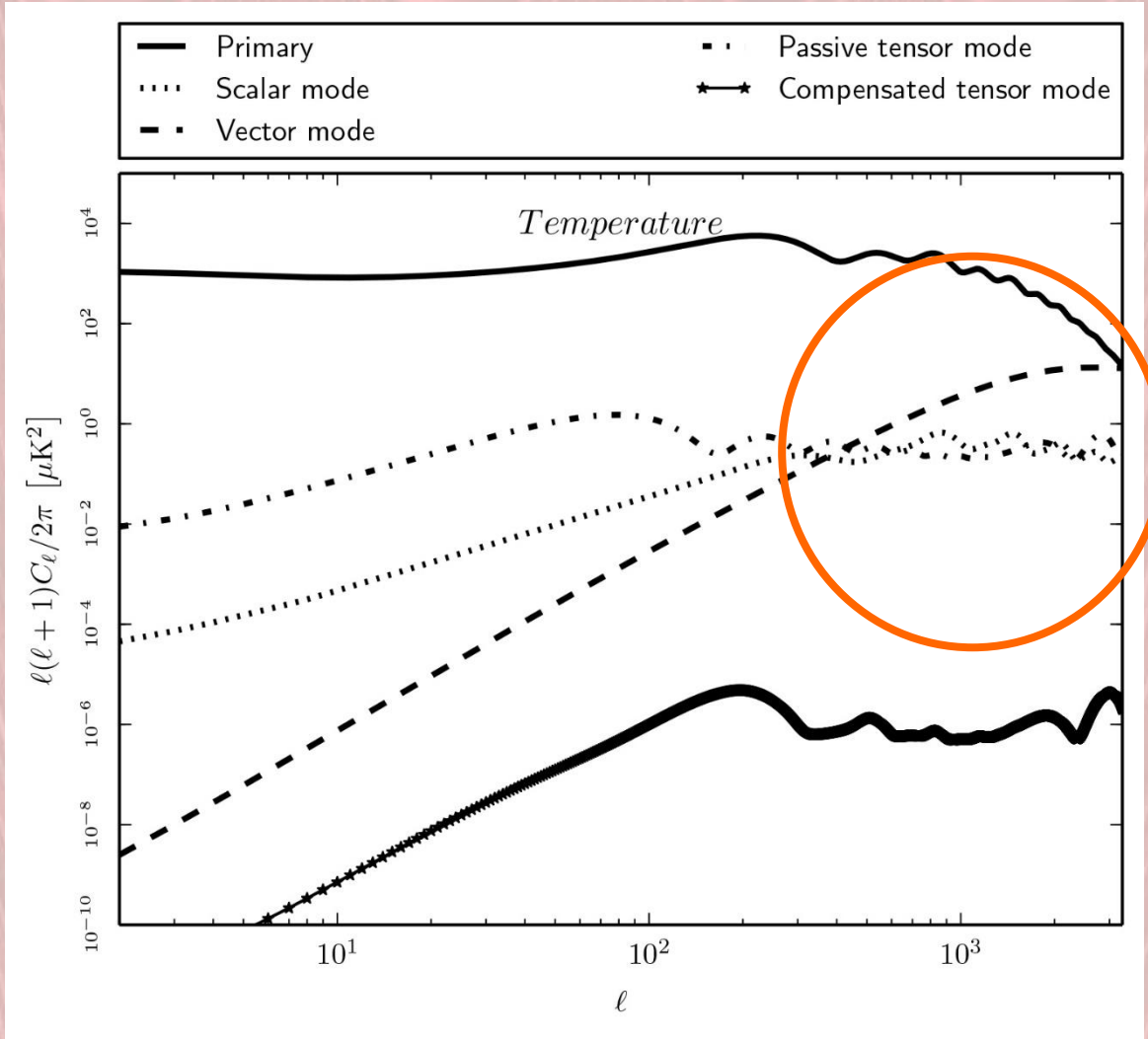

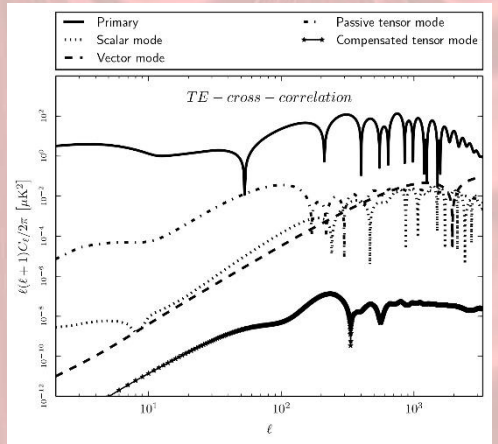

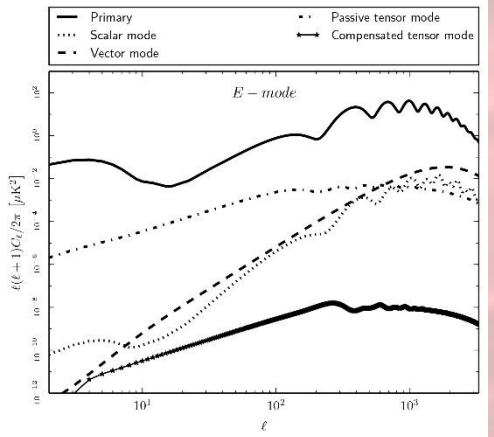

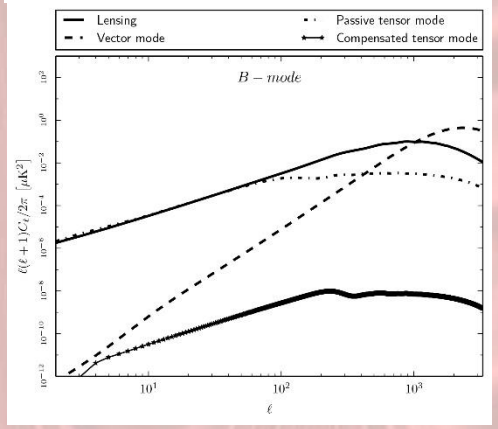

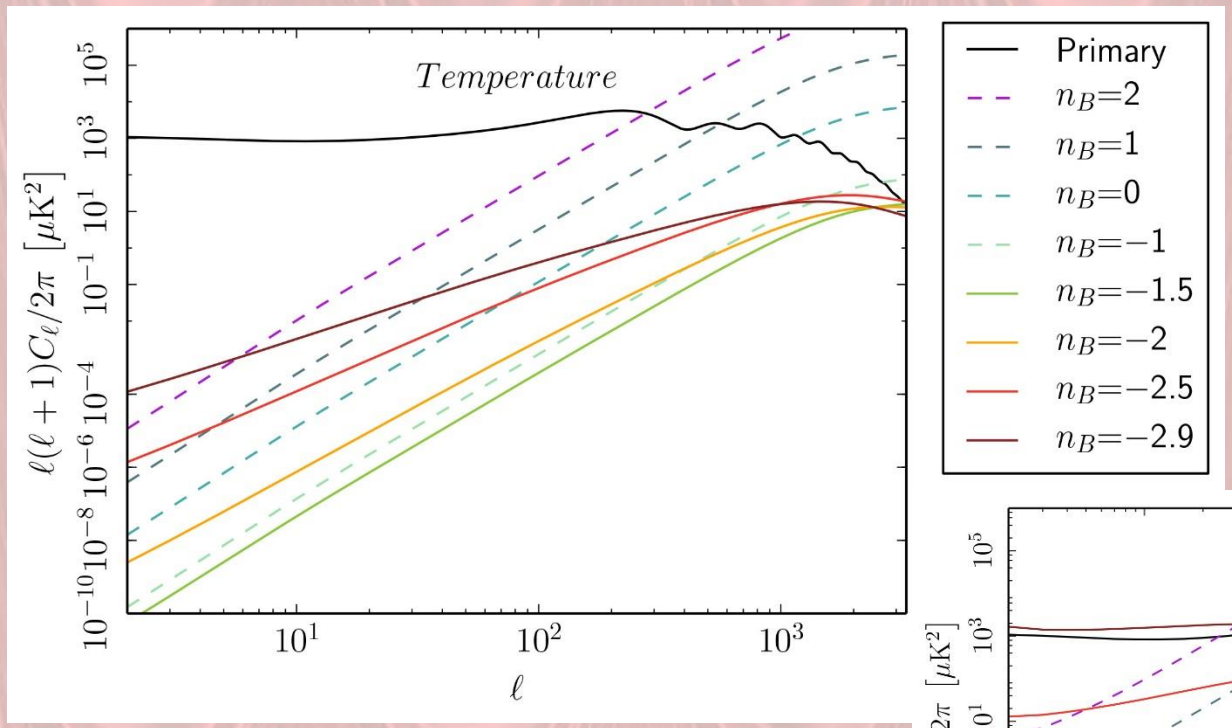

APS dependence on the PMF spectral index

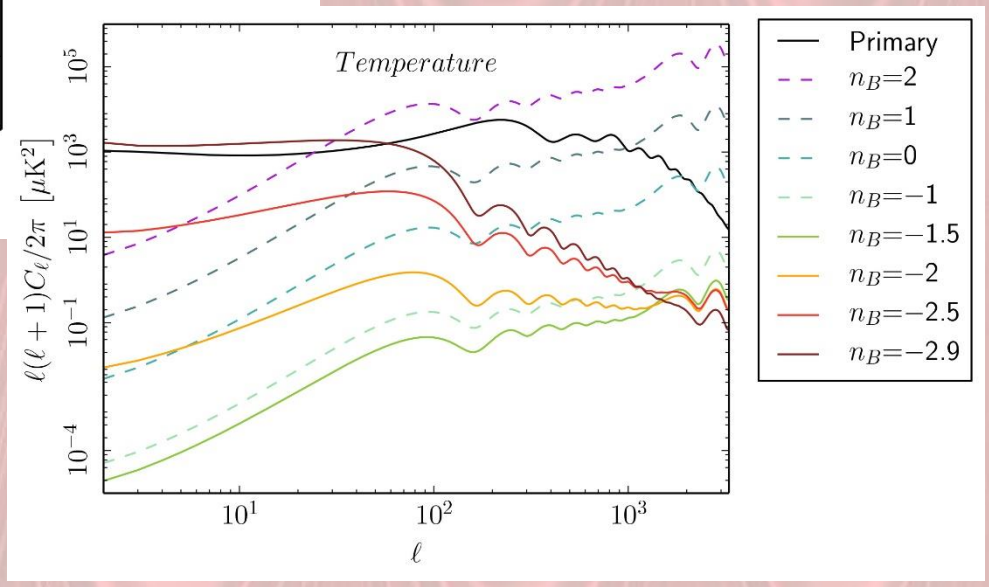

Behaviour driven by the PMF EMT spectrum:

- Indices >-1.5 show uniform shape with only variation in the amplitude , driven by the white noise spectra of PMF EMT
- Indices <-1.5 show a spectral shape which tilts accordingly to the infrared dominated behaviour of the PMF EMT spectra

HELICAL MAGNETIZED CMB ANGULAR POWER SPECTRA

MAXIMALLY HELICAL CASE

$$n_B = n_H$$

$$A_B = A_H$$

The presence of an extra term in the energy momentum tensor diminishes the PMF contribution for the helical case

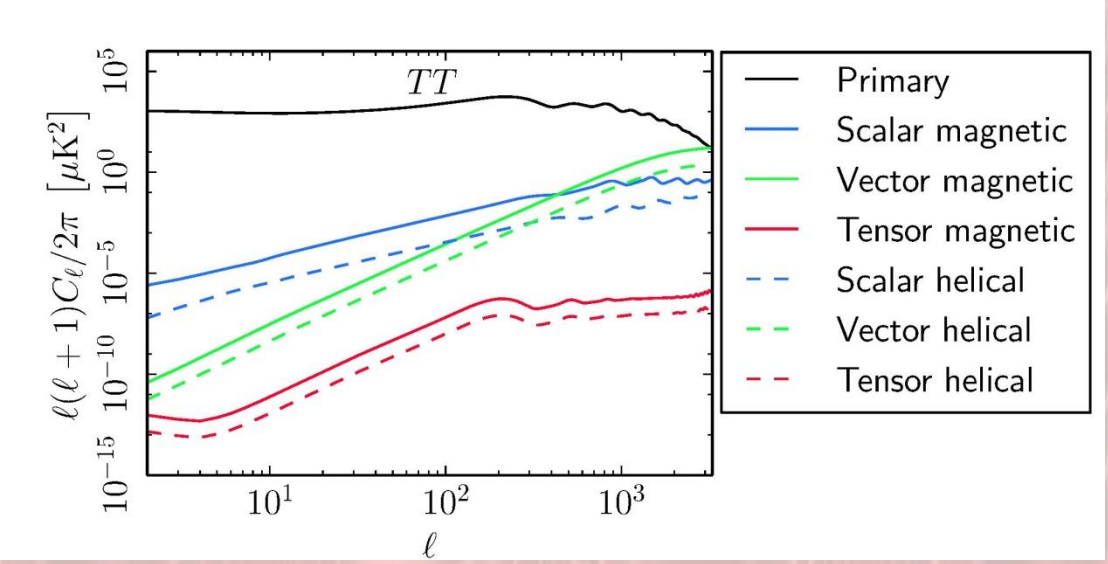

The antisymmetric part of the helical component generates non-zero ODD CMB cross correlator TB and EB

PLANCK 2015 CONSTRAINTS ON PMF

Astronomy & Astrophysics manuscript no. PMF˙Driver
February 5, 2015

Planck 2015 results. XIX. Constraints on primordial magnetic fields

Planck Collaboration: P. A. R. Ade[85], N. Aghanim[63], M. Arnaud[77], F. Arroja[70,83], M. Ashdown[73,6], J. Aumont[63], C. Baccigalupi[90], M. Ballardini[91,53,32], A. J. Banday[101,9], R. B. Barreiro[69], N. Bartolo[31,70], E. Battaner[103,104], K. Benabed[64,100], A. Benoît[61], A. Benoit-Lévy[25,64,100], J.-P. Bernard[101,9], M. Bersanelli[29,52], P. Bielewicz[101,9,90], A. Bonaldi[72], L. Bonavera[69], J. R. Bond[8], J. Borrill[14,95], F. R. Bouchet[63,93], M. Bucher[1], C. Burigana[51,33,53], R. C. Butler[51], E. Calabrese[98], J.-F. Cardoso[78,1,64], A. Catalano[79,76], A. Chamballu[77,16,63], H. C. Chiang[26,7], J. Chluba[24,75], P. R. Christensen[87,39], S. Church[97], D. L. Clements[59], S. Colombi[64,100], L. P. L. Colombo[23,73], C. Combet[79], F. Couchot[74], A. Coulais[76], B. P. Crill[73,11], A. Curto[8,69], F. Cuttaia[51], L. Danese[90], R. D. Davies[72], R. J. Davis[72], P. de Bernardis[28], A. de Rosa[51], G. de Zotti[48,90], J. Delabrouille[1], F.-X. Désert[57], J. M. Diego[69], K. Dolag[102,84], H. Dole[63,62], S. Donzelli[52], O. Doré[73,11], M. Douspis[63], A. Ducout[64,59], X. Dupac[41], G. Efstathiou[66], F. Elsner[25,64,100], T. A. Enßlin[84], H. K. Eriksen[67], J. Fergusson[12], F. Finelli[51,53], E. Florido[103], O. Forni[101,9], M. Frailis[50], A. A. Fraisse[26], E. Franceschi[51], A. Frejsel[87], S. Galeotta[50], S. Galli[64], K. Ganga[1], M. Giard[101,9], Y. Giraud-Héraud[1], E. Gjerløw[67], J. González-Nuevo[69,90], K. M. Górski[73,105], S. Gratton[73,66], A. Gregorio[30,50,58], A. Gruppuso[51], J. E. Gudmundsson[28], F. K. Hansen[67], D. Hanson[85,73,8], D. L. Harrison[66,73], G. Helou[11], S. Henrot-Versillé[74], C. Hernández-Monteagudo[13,84], D. Herranz[69], S. R. Hildebrandt[73,11], E. Hivon[64,100], M. Hobson[6], W. A. Holmes[73], A. Hornstrup[17], W. Hovest[84], K. M. Huffenberger[26], G. Hurier[63], A. H. Jaffe[58], T. R. Jaffe[101,9], W. C. Jones[28], M. Juvela[27], E. Keihänen[27], R. Keskitalo[14], J. Kim[84], T. S. Kisner[83], J. Knoche[84], M. Kunz[18,63,2], H. Kurki-Suonio[27,46], G. Lagache[4,63], A. Lähteenmäki[2,46], J.-M. Lamarre[76], A. Lasenby[6,73], M. Lattanzi[33], C. R. Lawrence[73], J. P. Leahy[72], R. Leonardi[41], J. Lesgourgues[99,88,75], F. Levrier[76], M. Liguori[31,70], P. B. Lilje[67], M. Linden-Vørnle[17], M. López-Caniego[41,69], P. M. Lubin[25], J. F. Macías-Pérez[79], G. Maggio[50], D. Maino[29,52], N. Mandolesi[51,33], A. Mangilli[63,74], P. G. Martin[6], E. Martínez-González[69], S. Masi[28], S. Matarrese[31,70,43], P. Mazzotta[37], P. McGehee[60], P. R. Meinhold[25], A. Melchiorri[28,54], L. Mendes[41], A. Mennella[35,52], M. Migliaccio[66,73], S. Mitra[58,73], M.-A. Miville-Deschênes[63,6], D. Molinari[99,51], A. Moneti[64], L. Montier[101,9], G. Morgante[51], D. Mortlock[58], A. Moss[92], D. Munshi[91], J. A. Murphy[86], P. Naselsky[87,39], F. Nati[28], P. Natoli[33,4,51], C. B. Netterfield[20], H. U. Nørgaard-Nielsen[17], F. Noviello[72], D. Novikov[82], I. Novikov[83,82], N. Oppermann[8], C. A. Oxborrow[17], F. Paci[90], L. Pagano[28,54], F. Pajot[63], D. Paoletti[51,53]*, F. Pasian[50], G. Patanchon[1], O. Perdereau[74], L. Perotto[79], F. Perrotta[90], V. Pettorino[45], F. Piacentini[28], M. Piat[1], E. Pierpaoli[25], D. Pietrobon[73], S. Plaszczynski[74], E. Pointecouteau[101,9], G. Polenta[4,49], L. Popa[65], G. W. Pratt[77], G. Prézeau[11,73], S. Prunet[64,100], J.-L. Puget[63], J. P. Rachen[21,84], R. Rebolo[68,15,40], M. Reinecke[84], M. Remazeilles[72,63,1], C. Renault[79], A. Renzi[34,55], I. Ristorcelli[101,9], G. Rocha[73,11], C. Rosset[1], M. Rossetti[29,52], G. Roudier[1,76,73], J. A. Rubiño-Martín[68,40], B. Ruiz-Granados[103], B. Rusholme[59], M. Sandri[51], D. Santos[79], M. Savelainen[27,46], G. Savini[89], D. Scott[22], M. D. Seiffert[73,11], E. P. S. Shellard[12], M. Shiraishi[31,70], L. D. Spencer[91], V. Stolyarov[6,73,96], R. Stompor[1], R. Sudiwala[91], R. Sunyaev[84,94], D. Sutton[66,73], A.-S. Suur-Uski[27,46], J.-F. Sygnet[64], J. A. Tauber[42], L. Terenzi[51,51], L. Toffolatti[10,68,51], M. Tomasi[29,52], M. Tristram[74], M. Tucci[18], J. Tuovinen[16], G. Umana[47], L. Valenziano[51], J. Valiviita[27,46], B. Van Tent[80], P. Vielva[68], F. Villa[51], L. A. Wade[73], B. D. Wandelt[64,100,31], I. K. Wehus[73], D. Yvon[18], A. Zacchei[50], and A. Zonca[29]

(*Affiliations can be found after the references*)

Preprint online version: February 5, 2015

ABSTRACT

We predict and investigate four types of imprint of a stochastic background of primordial magnetic fields (PMFs) on the cosmic microwave background (CMB) anisotropies: the impact of PMFs on the CMB temperature and polarization spectra, related to their contribution to cosmological perturbations; the effect on CMB polarization induced by Faraday rotation; magnetically-induced non-Gaussianities and related non-zero bispectra; and the magnetically-induced breaking of statistical isotropy. We present constraints on the amplitude of PMFs derived from different combinations of *Planck* data products, depending on the specific effect that is analysed. Overall, *Planck* data constrain the amplitude of PMFs to less than a few nanogauss, with different bounds depending on the considered model. In particular, individual limits coming from the analysis of the CMB angular power spectra, using the *Planck* likelihood, are $B_{1\,\mathrm{Mpc}} < 4.4$ nG (where $B_{1\,\mathrm{Mpc}}$ is the comoving field amplitude at a scale of 1 Mpc) at 95 % confidence level, assuming zero helicity, and $B_{1\,\mathrm{Mpc}} < 5.6$ nG when we consider a maximally helical field. For nearly scale-invariant PMFs we obtain $B_{1\,\mathrm{Mpc}} < 2.1$ nG and $B_{1\,\mathrm{Mpc}} < 0.7$ nG if the impact of PMFs on the ionization history of the Universe is included in the analysis. From the analysis of magnetically-induced non-Gaussianity we obtain three different values, corresponding to three applied methods, all below 5 nG. The constraint from the magnetically-induced passive-tensor bispectrum is $B_{1\,\mathrm{Mpc}} < 2.8$ nG. A search for preferred directions in the magnetically-induced passive bispectrum yields $B_{1\,\mathrm{Mpc}} < 4.5$ nG, whereas the the compensated-scalar bispectrum gives $B_{1\,\mathrm{Mpc}} < 3$ nG. The analysis of the Faraday rotation of CMB polarization by PMFs uses the *Planck* power spectra in *EE* and *BB* at 70 GHz and gives $B_{1\,\mathrm{Mpc}} < 1380$ nG. In our final analysis, we consider the harmonic-space correlations produced by Alfvén waves, finding no significant evidence for the presence of these waves. Together, these results comprise a comprehensive set of constraints on possible PMFs with *Planck* data.

Key words. magnetic fields – cosmology: cosmic background radiation – early Universe

* Corresponding author: D. Paoletti paoletti@iasfbo.inaf.it

1. Introduction

1.1. Cosmic magnetism

Magnetic fields are one of the fundamental and ubiquitous components of our Universe. They are a common feature of many

PART I: LIKELIHOOD

The predictions for the CMB angular power spectra are used to derive the constraints on PMF amplitude.

We explore the cosmological parameter space with the Markov Chain MonteCarlo code Cosmomc *(Bridle & Lewis 2002),* extendend in order to include PMF contributions *(Paoletti & Finelli 2010).*

In addition to the standard six standard model parameters (*baryon density, cold dark matter density, angular diameter distance horizon at recombination, spectral index, amplitude of primordial fluctuations, optical depth*) we vary the PMF amplitude and spectral index (for the case which include the passive mode also the additional parameter $\log(\tau_v/\tau_B)$)

We used the Planck 2015 likelihood with different combinations:

- **Planck TT / Planck TTTEEE** indicates the high-ell Planck likelihood, with either temperature only (TT) or temperature plus polarization (TTTEEE)
- **LowP** indicates the Planck low-ell likelihood based on the component separated Commander map for temperature and the LFI 70GHz maps cleaned with 30 GHz and 353 GHz for the polarization.

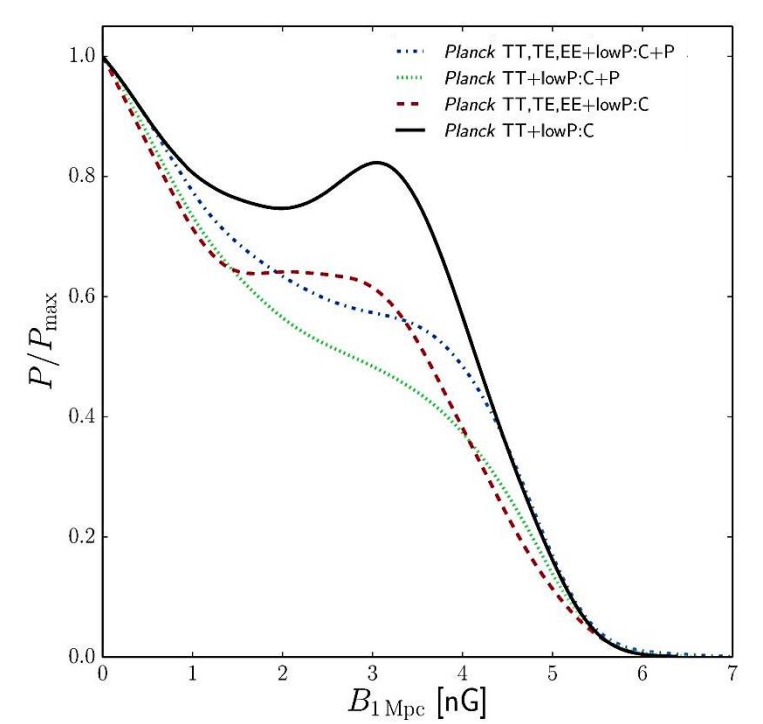

	$B_{1\,\rm Mpc}$/nG
TT,TE,EE+lowP: C	< 4.4
TT+lowP: C	< 4.4
TT,TE,EE+lowP: C+P . . .	< 4.5
TT+lowP: C+P	< 4.5
TT + $\tau_{\rm reion}$ prior: C+P	< 4.4

SPECTRAL INDEX	nG
n_B>0	$B_{1\,\rm Mpc}$< 0.55
n_B=2	$B_{1\,\rm Mpc}$<0.01
n_B=-2.9	$B_{1\,\rm Mpc}$<2.1

But we must be aware of degeneracies and of the number one enemy for PMF in the CMB anisotropies….

The impact of PMF is on small angular scales which are contaminated by astrophysical residuals.

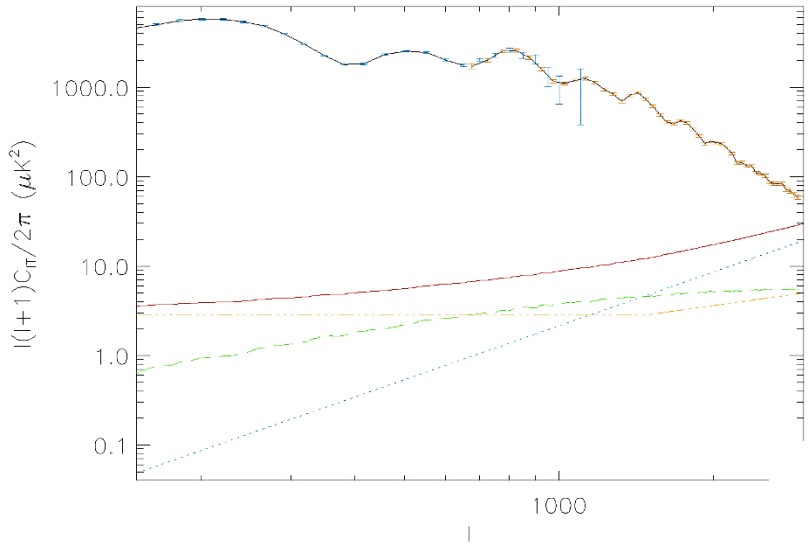

astrophysical contributions: SZ effect (dashed green line), the Poissonian term (dotted blue line), the clustering term (triple dot-dashed yellow line) and the solid red line represents the sum of the three. In the last panel the magnetic contributions including the uncorrelated sum of the two (dashed line) is compared with the total astropohysical contribution (solid line).

Paoletti & Finelli 2013

We use mock data as an example

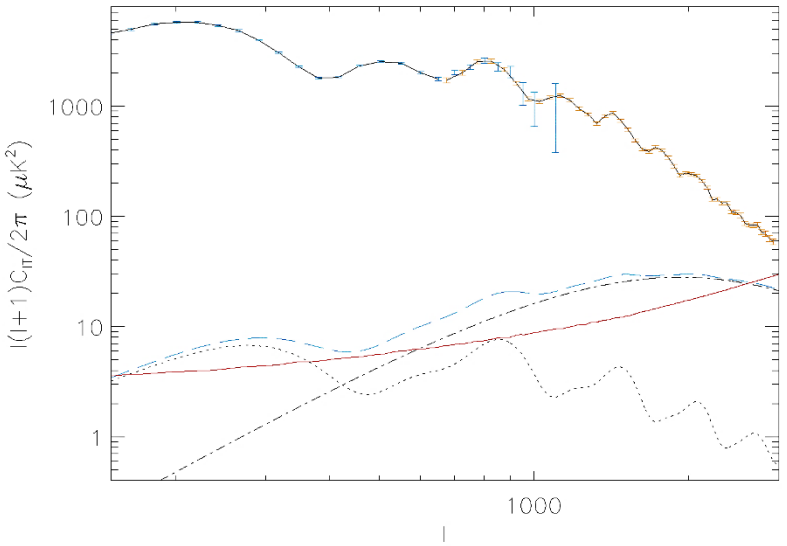

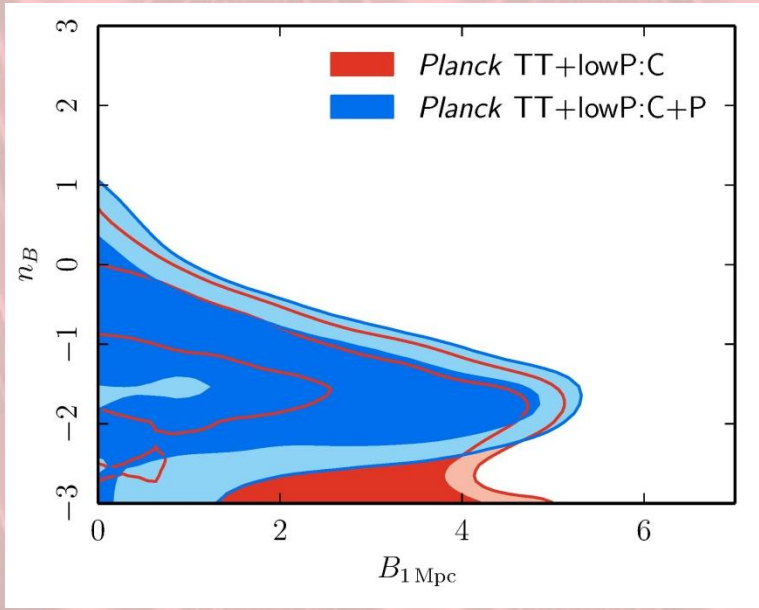

Strong degeneracy between the amplitude and the spectral index

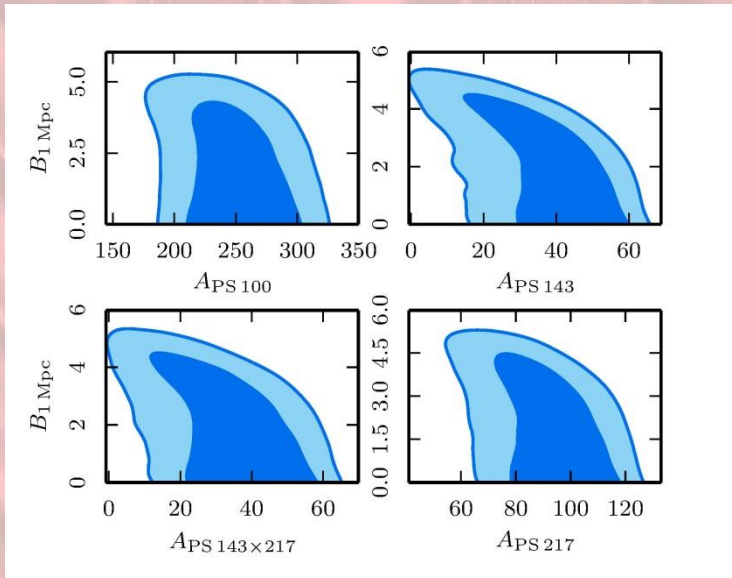

Degeneracy between the amplitude and the foreground residual parameters for the Poissonian terms

Compare with
Planck 2013 results: $B_{1\,\mathrm{Mpc}} < 4.1\,\mathrm{nG}$ (95 % CL, PLANCK TT+lowP)

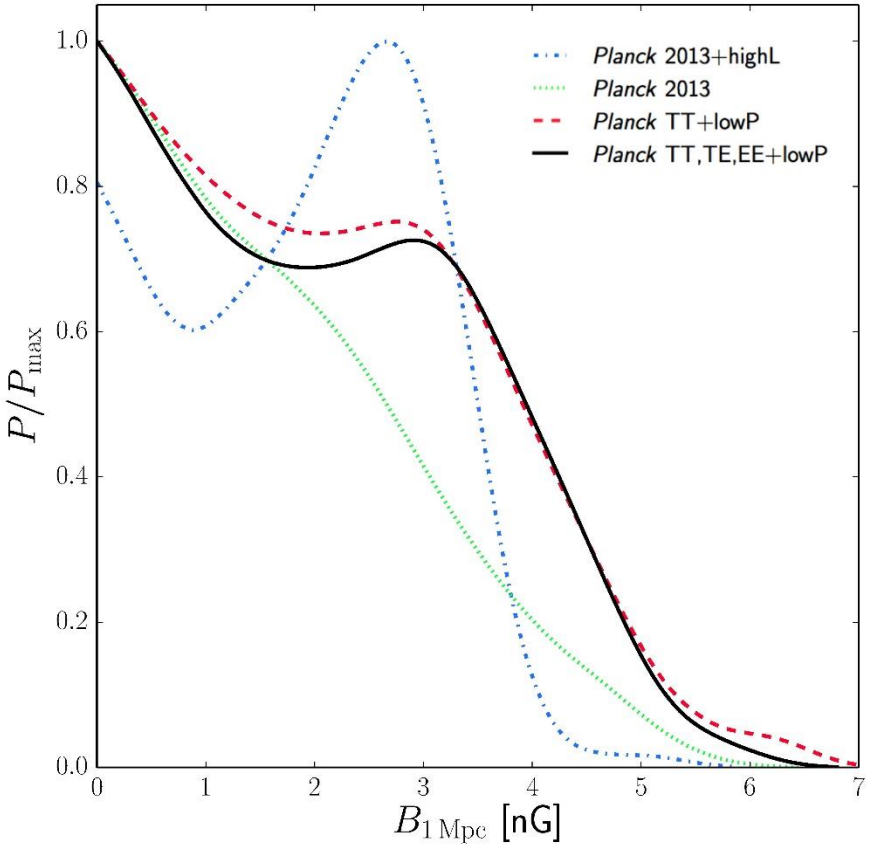

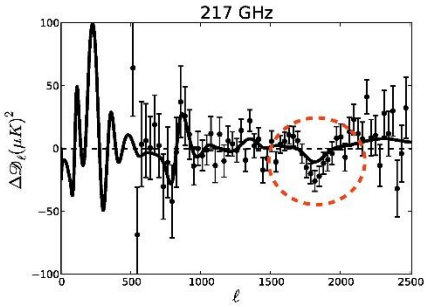

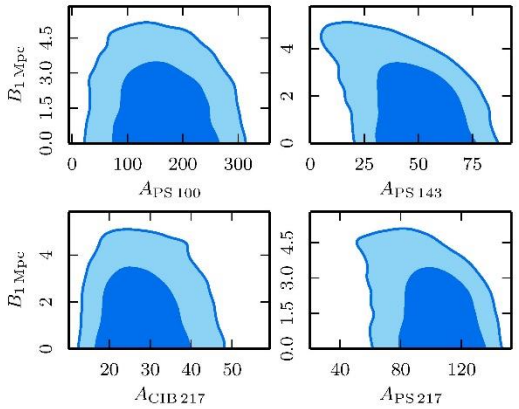

Correlation with foregrounds for Planck 2013

planck

F. Finelli, Nordita, 22 June 2015

CONSTRAINTS FOR HELICAL FIELDS

MAXIMALLY HELICAL

The constraint on PMF amplitude with an helical component is

$$B_{1\,\mathrm{Mpc}} < 5.6\ \mathrm{nG}$$

Which can be translated into a contraint on th amplitude of the helical component

$$\mathcal{B}_{1\,\mathrm{Mpc}} < 4.6\ \mathrm{nG}$$

The constrains are derived with the Planck TT and lowP likelihood and they include only the even-power spectra

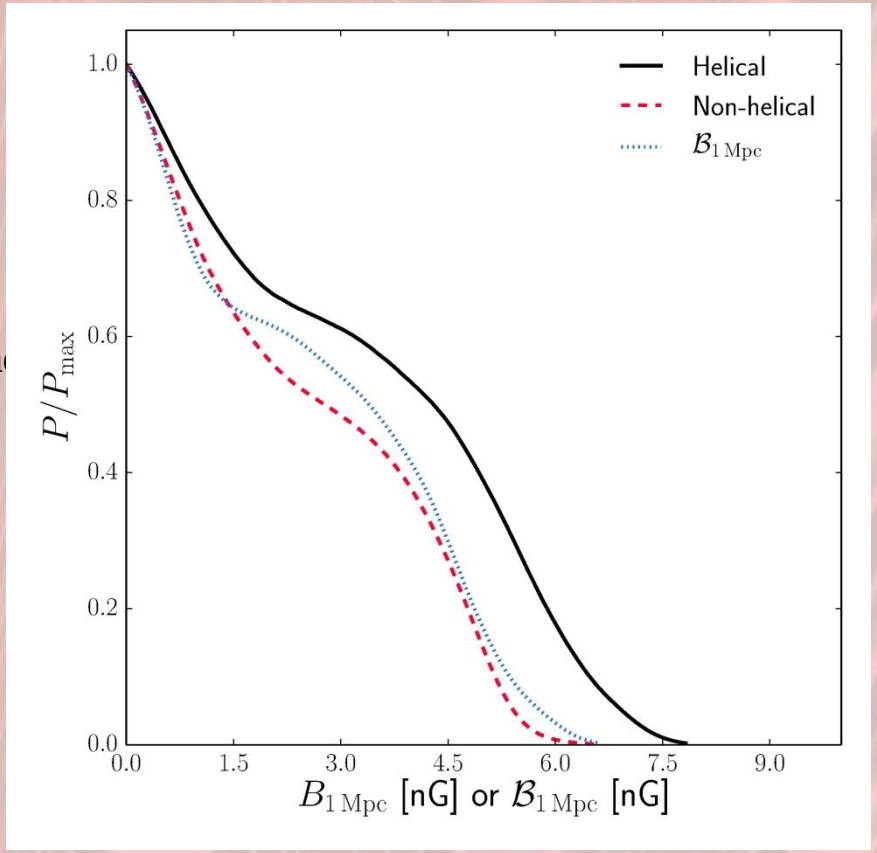

JOINT PLANCK+BICEP 2/KECK Array

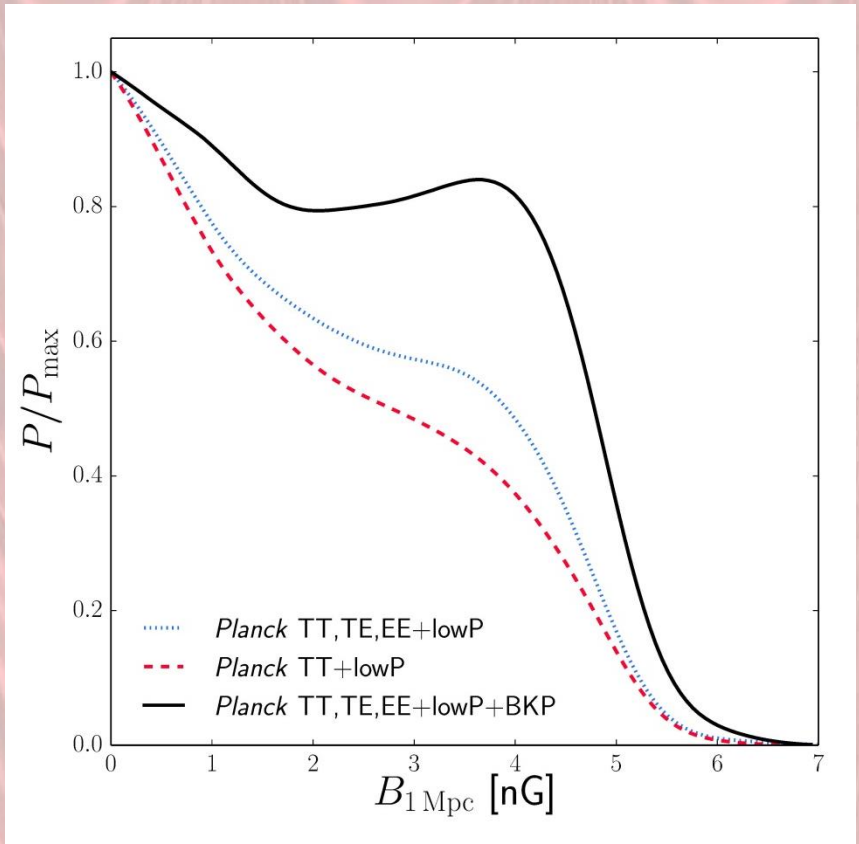

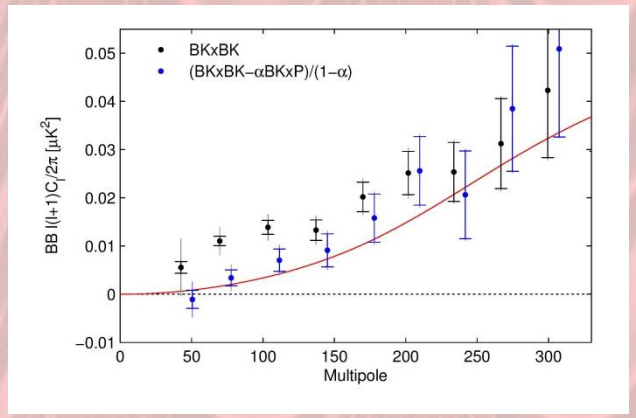

$$B_{1\,\mathrm{Mpc}} < 4.7\,\mathrm{nG}$$

IMPACT OF THE IONIZATION HISTORY

The presence of PMF modifies the ionization history. This is due to the injection of energy into the plasma caused by the dissipation of the PMF. In particular we have two main mechanisms *(Sethi & Subramanian 2005, Chluba et al. 2015, Kunze & Komatsu 2015):*

AMBIPOLAR DIFFUSION ⟷ **MHD DECAYING TURBULENCE**

$$\Gamma_{\rm am} \approx \frac{(1-X_{\rm p})}{\gamma X_{\rm p}\,\rho_{\rm b}^2}\frac{|(\nabla\times B)\times B|^2}{16\pi^2}$$

$$\Gamma_{\rm turb} = \frac{3m}{2}\frac{\left[\ln\left(1+\frac{t_i}{t_{\rm d}}\right)\right]^m}{\left[\ln\left(1+\frac{t_i}{t_{\rm d}}\right)+\frac{3}{2}\ln\left(\frac{1+z_i}{1+z}\right)\right]^{m+1}}H(z)\,\rho_{\rm B}(z)$$

$$\frac{dT_e}{dt} = -2HT_e + \frac{8\sigma_T N_e\,\rho_\gamma}{3m_e c N_{\rm tot}}(T_\gamma - T_e) + \frac{\Gamma}{(3/2)kN_{\rm tot}}$$

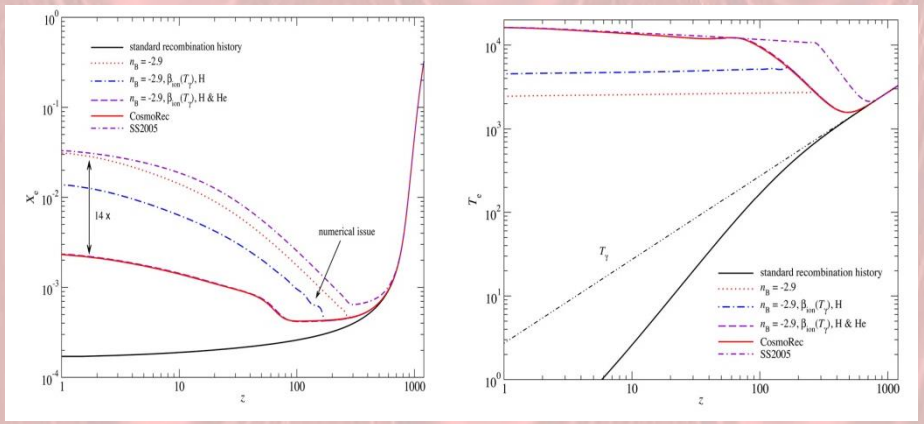

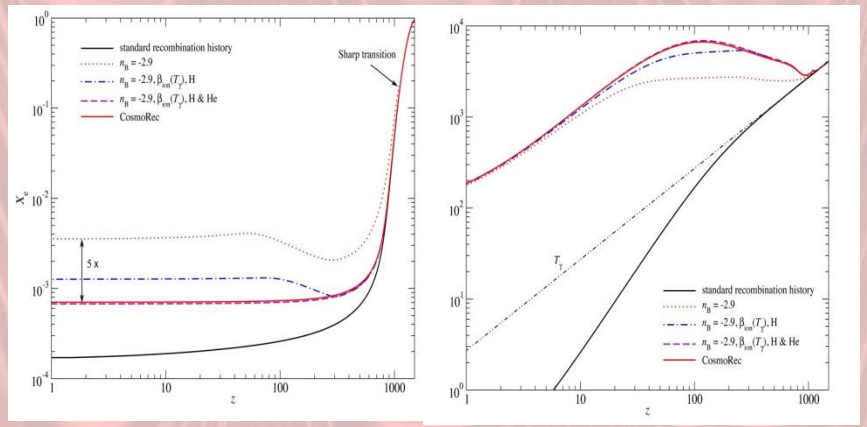

Chluba, Paoletti, Finelli and Rubino-Martin 2015

Chluba, Paoletti, Finelli & Rubino-Martin 2015

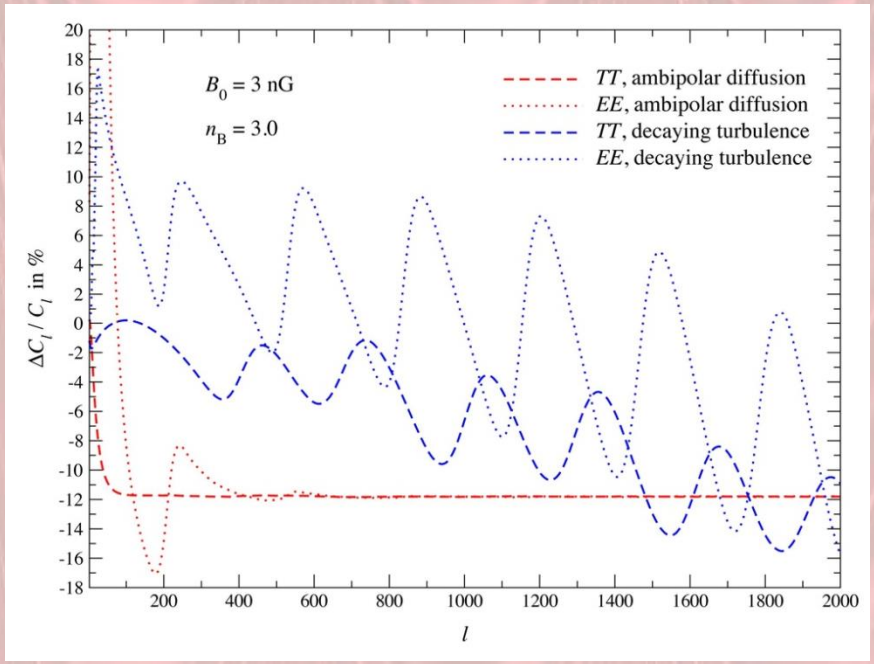

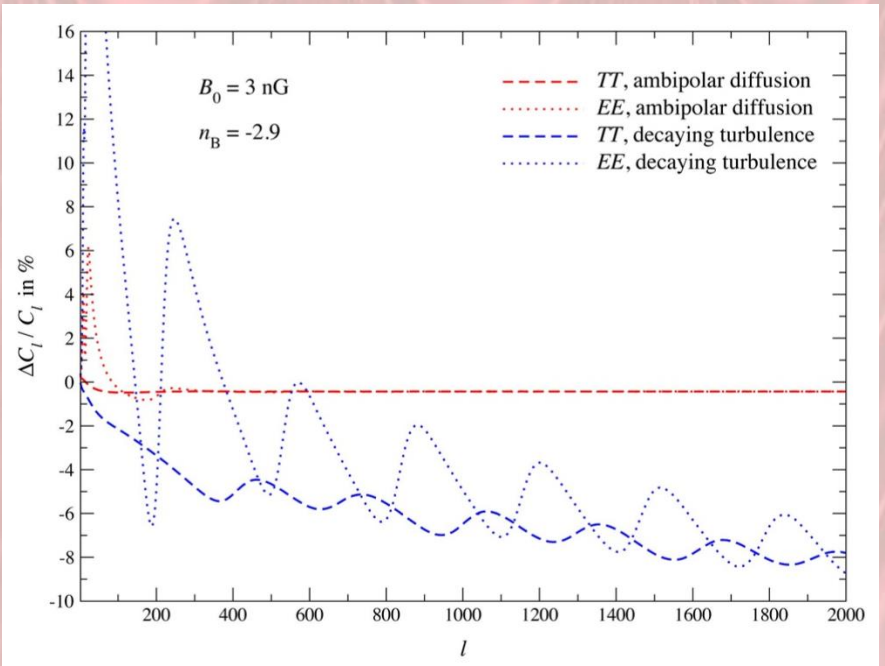

Very large effect for blue spectral indices

For blue indices the ambipolar diffusion term dominates whereas red indices are dominated by MHD decaying turbulence

Using this effect the Planck TT+lowP constraints the smoothed amplitude (1 Mpc) of scale invariant PMF ($n_B = -2.9$) are less than 1 nG

PART II:
NON-GAUSSIANITIES

THE CMB IS NOT ONLY THE TWO POINT CORRELATION FUNCTION….

PMF modelled as a stochastic background have a fully non-Gaussian impact on CMB anisotropies. PMF generates non-zero three point correlation function (bispectrum) and four point correlation function (trispectrum)

The constraints derived with the non-Gaussianity measurements are complementary to the ones derived with the Planck likelihood.

The angular power spectrum is the two point correlation function and it depends on the fourth power of the fields.

Similarly the magnetically induced bispectrum, which is the three point correlation function, depends on the sixth power of the fields!

As for the two point correlation function also for non-Gaussianity analysis we can consider different initial conditions and different modes.

Brown & Crittenden 2005, Brown 2008, Seshadri & Subramanian 2009, Caprini, Finelli, Paoletti & Riotto 2009, Trivedi, Subramanian & Seshadri 2010, Shiraishi et Al. 2011, Shiraishi et Al. 2011/2, Trivedi, Subramanian & Seshadri 2011, Shiraishi et Al.2012…….

In Planck 2015 results XIX we have considered three cases:

- Tensor passive bispectrum
- Anisotropic bispectrum for passive modes
- Compensated scalar bispectrum

TENSOR PASSIVE BISPECTRUM

The tensor passive mode is the dominant contribution to the large scale angular power spectrum for scale invariant PMF (n_B=-2.9).

We have considered the magnetized passive tensor bispectrum for l<500 and the squeezed limit configuration in which the passive bispectrum is amplified.

$$\ell_1 \ll \ell_2 \approx \ell_3$$

$$A_{\rm bis} \equiv \left(\frac{B_{1\,\rm Mpc}}{3\,\rm nG}\right)^6 \left[\frac{\ln(\tau_\nu/\tau_B)}{\ln(10^{17})}\right]^3 ,$$

Optimal estimator in separable modal methodology *(Shiraishi et. Al 2014, Planck Coll. 2014, Fergusson 2014,Liguori et al. 2014)*
The limits on the bispectrum amplitude can be translated into limits for the fields

SMICA FG cleaned maps T and E for PMF generated at the Grand Unification scale with n_B=-2.9

$$B_{1\,Mpc} < 2.8\,nG$$

ANISOTROPIC BISPECTRUM FOR SCALAR PASSIVE

Considering the curvature perturbations induced by passive modes

$$\zeta_{\boldsymbol{k}} \approx 0.9 \ln\left(\frac{\tau_\nu}{\tau_B}\right) \frac{1}{4\pi\rho_{\gamma,0}} \sum_{ij}\left(\hat{k}_i\hat{k}_j - \frac{1}{3}\delta_{ij}\right)\int \frac{\mathrm{d}^3\boldsymbol{k}'}{(2\pi)^3} B_i(\boldsymbol{k}')\, B_j(\boldsymbol{k}-\boldsymbol{k}')\,.$$

PMF produce non-vanishing bispectrum of direction-dependence

Legendre Polynomial

$$\langle\zeta(\vec{k}_1)\zeta(\vec{k}_2)\zeta(\vec{k}_3)\rangle = \sum_L c_L\left(P_L(\hat{\mathbf{k}}_1\cdot\hat{\mathbf{k}}_2)P_\Phi(k_1)P_\Phi(k_2) + 2\,\text{perm}\right)$$

The zeroth and the second expansion coefficients are related to the amplitude of magnetic fields:

$$c_0 \approx -2\times10^{-4}\left(\frac{B_{1\text{Mpc}}}{\text{nG}}\right)^6,$$

$$c_2 \approx -2.8\times10^{-3}\left(\frac{B_{1\text{Mpc}}}{\text{nG}}\right)^6$$

Constraints on the amplitude for B_{1MPC} [nG] with n_B=-2.9 generated at the GUT scale for the four component separation maps available in Planck 2015

	SMICA	NILC	SEVEM	Commander
$B_{1\,\text{Mpc}}/\text{nG}$ . . .	< 4.5	< 4.9	< 5.0	< 5.0

COMPENSATED SCALAR MAGNETIZED BISPECTRUM

We derived the analytical magnetized compensated scalar bispectrum on large angular scales. The temperature anisotropy for PMF can be written as

$$\frac{\Theta_\ell^{(0)}(\eta_0,\mathbf{k})}{2\ell+1} = \frac{\alpha}{4}\Omega_{\rm B}(\mathbf{k}) j_\ell(\mathbf{k}(\eta_0-\eta_{\rm dec}))\,,$$

The magnetized bispectrum depends on the magnetic energy density bispectrum

$$\langle \rho_B(\mathbf{k})\rho_B(\mathbf{q})\rho_B(\mathbf{p})\rangle = \frac{1}{(8\pi)^3}\int \frac{d^3\tilde{k}\,d^3\tilde{q}\,d^3\tilde{p}}{(2\pi)^9}\langle B_i(\tilde{\mathbf{k}})B_i(\mathbf{k}-\tilde{\mathbf{k}})B_j(\tilde{\mathbf{q}})B_j(\mathbf{q}-\tilde{\mathbf{q}})B_l(\tilde{\mathbf{p}})B_l(\mathbf{p}-\tilde{\mathbf{p}})\rangle\,.$$

Contrary to the passive case for compensated mode there is no a-priori dominant geometrical configuration

By the comparison of the bispectrum and the spectrum it is possible to derive an effective f_{nl} in the local configuration to be compared with the measured one (SMICA KSW) to constrain PMF

$$f_{\rm NL}^{eff} \simeq \frac{3\pi^9\,\alpha^3}{2304\,\mathcal{A}^2}\frac{n_{\rm B}(n_{\rm B}+3)^2}{2n_{\rm B}+3}\frac{\langle B^2\rangle^3}{\rho_{rel}^3} \simeq 1.2\times10^{-3}\,(n_{\rm B}+3)^2\left(\frac{\langle B^2\rangle}{(10^{-9}\,{\rm G})^2}\right)^3\,.$$

$$B_{1\,{\rm Mpc}} < 3.0\,{\rm nG}\ (95\%{\rm CL}, n_{\rm B}=-2.9)$$

PART III:
FARADAY ROTATION

FARADAY ROTATION

The presence of PMF induces a rotation of the polarization plane of CMB anisotropies rotating *E*-mode polarization into *B*-mode and vice versa. The Faraday depth is given by

$$\Phi = K \int n_{\rm e}(x, \boldsymbol{n})\, B_{\parallel}(x, \boldsymbol{n})\, {\rm d}\boldsymbol{x}.$$

B and E mode polarization rotated spectra

$$C_\ell^{BB} = N_\ell^2 \sum_{\ell_1 \ell_2} \frac{(2\ell_1+1)(2\ell_2+1)}{4\pi(2\ell+1)} N_{\ell_2}^2\, K(\ell,\ell_1,\ell_2)^2\, C_{\ell_2}^{EE}\, C_{\ell_1}^{\alpha}\, \left(C_{\ell_1 0 \ell_2 0}^{\ell 0}\right)^2$$

$$C_\ell^{EE} = N_\ell^2 \sum_{\ell_1 \ell_2} \frac{(2\ell_1+1)(2\ell_2+1)}{4\pi(2\ell+1)} N_{\ell_2}^2\, K(\ell,\ell_1,\ell_2)^2\, C_{\ell_2}^{BB}\, C_{\ell_1}^{\alpha}\, \left(C_{\ell_1 0 \ell_2 0}^{\ell 0}\right)^2$$

$$C_\ell^{\Phi} \approx \frac{9\ell(\ell+1)}{(4\pi)^3 e^2} \frac{B_\lambda^2}{\Gamma(n_B+3/2)} \left(\frac{\lambda}{\eta_0}\right)^{n_B+3} \int_0^{x_{\rm D}} {\rm d}x\, x^{n_B}\, j_\ell^2(x).$$

$$C_\ell^{\alpha} = \nu_0^{-4} C_\ell^{\Phi},$$

Strong frequency dependence! Lower frequencies are more affected by Faraday rotation

The *EE* mode from Planck 70 GHz (2<l<29) spectrum has been used to derive the expected *BB* rotated mode. Comparison with measured *B*-modes at 70 GHz computing the minimum χ^2.

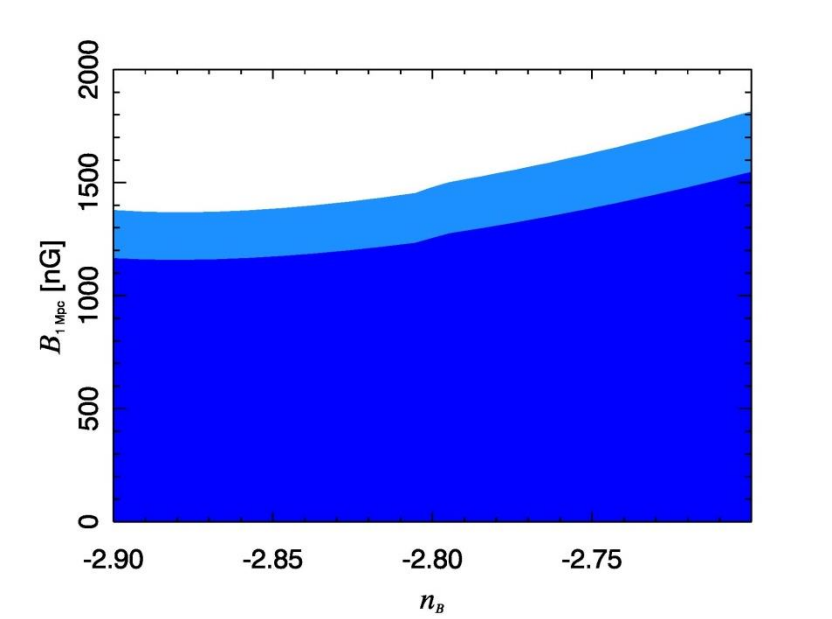

$$B_{1\,\mathrm{Mpc}} < 1380\ \mathrm{nG}$$

Estimate of the Galactic contribution, subdominant for our data

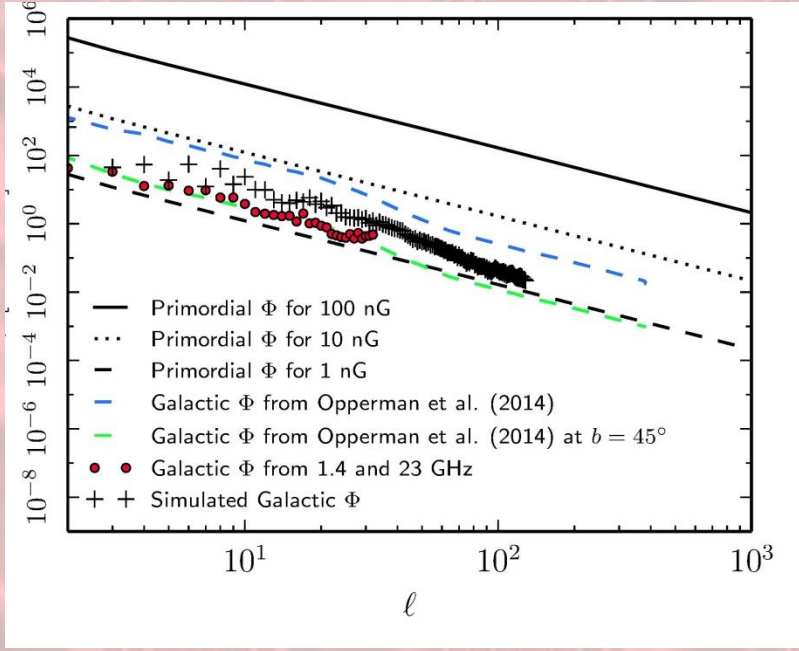

CONCLUSIONS

Ever increasing accuracy of cosmological data allows to strongly constraints PMF amplitude and in particular CMB data have been proven to be one of the best laboratory to investigate and constrain PMF

A stochastic background of PMF leaves different peculiar imprints on CMB anisotropies through scalar, vector and tensor contributions both in temperature and polarization

- At the CMB angular power spectrum level the stronger contribution is given by magnetically induced vector perturbations on small angular scales. For scale invariant spectral index it is relevant also the contribution of the passive tensor mode on large angular scales. The impact of PMF on the ionization history also leads to tight constraints and looks very promising in the perspective of new data in polarization. Overall, the Planck 2015 constraints based on the power spectrum are at level on nG.

- A stochastic background of PMF has a fully non-Gaussian impact on CMB anisotropies generating non-zero higher statistical moments. In particular, PMF generates a non-zero bispectrum with different modes and initial conditions. Using different bispectra and different techniques Planck 2015 has show that non-Gaussianity constraints are very competitive with likelihood ones.

- PMF induce a Faraday rotation of the CMB anisotropy in polarization generating a B-mode polarization from the primary E-mode. Using the BB-spectrum available from the 70GHz Planck likelihood it is possible to give constraints on PMF. These constraints are based on a very limited range of multipoles where the signal is subdominant and therefore are larger with respect to the other methods.

Model/Dataset/Method	nG
Planck TT+lowP	$B_{1\ Mpc} < 4.4$
Planck TT,TE,EE+lowP	$B_{1\ Mpc} < 4.4$
$n_B > 0$	$B_{1\ Mpc} < 0.55$
$n_B = 2$	$B_{1\ Mpc} < 0.01$
$n_B = -2.9$	$B_{1\ Mpc} < 2.1$
Helical PMF	$B_{1\ Mpc} < 5.6$
Planck+BICEP 2/KECK ARRAY	$B_{1\ Mpc} < 4.7$
Impact on the ionization history	$B_{1\ Mpc} < 1$
Passive tensor mode bispectrum $n_B = -2.9$	$B_{1\ Mpc} < 2.8$
Passive anisotropic bispectrum $n_B = -2.9$	$B_{1\ Mpc} < 4.5$
Scalar compensated bispectrum $n_B = -2.9$	$B_{1\ Mpc} < 3.0$
Faraday rotation	$B_{1\ Mpc} < 1380$

PART OF THE WORK PRESENTED HAVE BEEN DONE IN THE FRAMEWORK OF THE PLANCK COLLABORATION

Planck is a project of the European Space Agency, with instruments provided by two scientific Consortia funded by ESA member states (in particular the lead countries: France and Italy) with contributions from NASA (USA), and telescope reflectors provided in a collaboration between ESA and a scientific Consortium led and funded by Denmark.


Thank you